nature reviews earth & environment

https://doi.org/10.1038/s43017-026-00818-7

Review article

Check for updates

Importance, drivers and trends of inland water greenhouse gas emissions

Ronny Lauerwald[1] ✉, David Bastviken[2], Tom Battin[3], Philippe Ciais[4], Hanqin Tian[5], George H. Allen[6], Gwenaël Abril[7], Núria Catalan[8], Bridget R. Deemer[9], Alessandra Marzadri[10], Yves Prairie[11], Suzanne E. Tank[12], Qianlai Zhuang[13], Lishan Ran[14], Josep G. Canadell[15] & Pierre Regnier[16]

Abstract

Inland waters are major sources of greenhouse gases (GHGs) to the atmosphere. In this Review, we compile and reconcile current global estimates of CO_2, CH_4 and N_2O emissions from inland waters and place them in the context of the global GHG budget. Estimates indicate total inland water emissions of approximately 8.2 (6.5–10.6; 90% CI) Pg CO_2-eq. yr^{-1} over a 100-year time horizon, despite inland waters only covering less than 3% of the land surface. Mapping of global emission patterns reveals that the largest emitters of GHGs are low-latitude river networks and the numerous small lakes of the Northern Hemisphere. High latitudes, the tropics and very small water bodies have a major role in global fluxes but remain under-represented in observational datasets. Drawing on modelling and budget analyses, we estimate that emissions have increased by approximately 2.8 (2.3–3.5; 90% CI) Pg CO_2-eq. yr^{-1} since the Industrial Revolution, equivalent to an offset of approximately one-third of the land carbon sink. Global inland water GHG emissions are expected to keep increasing throughout the twenty-first century, mainly driven by climate change, but pollution control and careful dam planning could help to limit this increase.

Sections

Introduction

Inland waters in the greenhouse gas budget

Global spatial patterns and hot spots

The sources and sinks of emitted GHGs

Evolution of emissions under global change

Summary and future perspectives

A full list of affiliations appears at the end of the paper. ✉e-mail: ronny.lauerwald@inrae.fr

Introduction

Inland waters, including streams, rivers, lakes and reservoirs, are important sources of greenhouse gases (GHGs) to the atmosphere. Estimates indicate that the combined GHG emissions from inland waters is 8.3 (5.7–12.7; interquartile range (IQR)) Pg CO_2-eq. yr^{-1} for a 100-year time horizon[1], approximately one-fourth that of fossil CO_2 emissions[2].

Since the milestone paper by Cole et al.[3] in 2007, the role of inland waters as major GHG sources has been increasingly recognized in global climate assessments, including those of the Intergovernmental Panel on Climate Change (IPCC) and the Global Carbon Project[2,4,5]. Although uncertainties persist, advances in research methodologies have notably increased our understanding of global flux estimates. Over the past two decades, the number of published estimates of inland water GHG emissions has increased considerably, integrating more robust field data and sophisticated approaches such as machine learning and process-based modelling[6]. Additionally, spatially explicit estimates provide higher-resolution maps of emissions, enabling their use in spatialized GHG budgets[4,7,8] and as prior estimates for atmospheric inversion models[9]. Moreover, the development of process-based[10–12] and advanced empirical models[13] has facilitated simulations of inland water GHG dynamics in response to climate change and direct anthropogenic perturbations such as river damming and water pollution.

In this Review, we first assess the current state of knowledge on inland water GHG emissions and their relevance to global-scale GHG budgets. Next, we summarize existing spatially explicit estimates to generate global emission maps, identifying hot spots and key drivers of GHG emissions. We further highlight regions that have a substantial role in global fluxes yet remain under-represented in observational datasets. Subsequently, we address fundamental questions regarding the sources of GHG emissions, including the extent to which GHGs are produced within inland waters, and the proportion of emissions that originate from external inputs such as from groundwater, adjacent soils and wetlands. We then explore the implications of environmental change for inland water GHG emissions, identifying the primary drivers of long-term emission trends and assessing how emissions have been influenced by anthropogenic perturbations associated with land use change, water pollution, river damming, atmospheric CO_2 increase and climate change relative to pre-industrial conditions. Lastly, we discuss the probable future trajectories of emissions over the twenty-first century.

Inland waters in the greenhouse gas budget

Inland waters are an important but poorly constrained component of the global GHG budget, with emissions that are sizeable compared with many other major sources and sinks (Table 1). As part of the second phase of the REgional Carbon Cycle Assessment and Processes initiative, which aimed to improve the quantification and understanding of GHG budgets across ten world regions, Lauerwald et al.[1] synthesized existing estimates of inland water GHG emissions to provide consistent and harmonized flux estimates for inclusion in these regional budgets. In the present Review, we update that synthesis by incorporating and focusing on the most recent estimates of inland water GHG emissions.

CO_2 emissions from inland waters

The extent of global CO_2 emissions from inland waters remains relatively uncertain. Although it is widely accepted that inland water emissions of CO_2 predominantly come from streams and rivers, existing estimates vary by one order of magnitude (Table 1, and see Supplementary Table 1 for details). In the latest estimate[14], which falls at the upper end of the range of previous estimates, CO_2 partial pressure was measured directly rather than inferred from alkalinity and pH, an important advance over previous work[15,16], which often overestimated fluxes from acidic freshwaters[17]. Despite these uncertainties, there is a consensus that inland water CO_2 emissions are substantial relative to land and ocean sinks of anthropogenic CO_2 (Table 1), even though inland waters cover only <1% of Earth's surface and <3% of the land surface[1]. However, inland water CO_2 emissions are predominantly natural in origin, whereas land and ocean carbon sinks largely represent a perturbation driven by anthropogenic CO_2 emissions. Although inland water CO_2 emissions mostly reflect a natural background flux sustained by carbon originating from terrestrial and wetland ecosystems, they are also influenced by anthropogenic perturbations of these ecosystems[10,18]. Furthermore, inland water CO_2 emissions are implicitly included in estimates of land CO_2 uptake based on atmospheric inversions[19]. Improved assessment of inland water CO_2 emissions is therefore key to a better understanding of the dynamics behind the land CO_2 sink and ultimately projecting its future capacity to offset anthropogenic CO_2 emissions.

CH_4 emissions from inland waters

Two global estimates of inland water CH_4 emissions have been published since Lauerwald et al.[1]. One of these studies examined riverine CH_4 emissions[20], whereas the other investigated emissions from lakes, including reservoirs[11]. The river analysis, which is perhaps the most advanced at present in terms of using empirical databases and spatial extrapolation methods, estimated river emissions of 27.9 Tg CH_4 yr^{-1}, a value similar to that reported by Lauerwald et al.[1] (23 Tg CH_4 yr^{-1}). By contrast, recent global estimates of CH_4 emissions from lakes[8,9,11] suggest a value of 42 (22–81; min–max) Tg CH_4 yr^{-1}, substantially lower than the earlier estimate reported by Lauerwald et al.[1] (66 (32–127; min–max) Tg CH_4 yr^{-1}). This downward revision reflects a broader trend of lower global emission estimates since 2020[6], probably driven by broader observational coverage[21] and by upscaling approaches that better account for seasonal variability[9]. Lower estimates are further supported by atmospheric inversion models, which indicate that previous estimates of inland water emissions were overestimated[5].

Nevertheless, inland waters are the second largest natural source of CH_4 after wetlands, and in contrast to CO_2, lakes contribute a major part of that flux (Table 1). In total, the emissions from reservoirs are lower than those from natural lakes but are still disproportionately important considering that reservoirs constitute a new source of CH_4 to the atmosphere and account for approximately one-tenth of the global surface area of lakes. Moreover, emissions from dam outlets, which are not accounted for in most estimates, are potentially higher than the emission from the water surface[22]. When expressed as CO_2 equivalents using a 100-year global warming potential (GWP100, 27 kg CO_2-eq. per kg CH_4), inland water CH_4 emissions of 2.6 (2.1–3.4; here and wherever not indicated otherwise, uncertainty range is reported as 5th and 95th percentiles of confidence interval (90% CI)) Pg CO_2-eq. yr^{-1} are lower but of a similar order of magnitude to inland water CO_2 emissions.

N_2O emissions from inland waters

Extending previous work[23] that examined the dynamics of riverine N_2O emissions, N_2O emissions have been modelled from reservoirs and lakes. In one study[12], unlike other estimates of riverine N_2O emissions, the authors explicitly quantified the N_2O emissions from headwater streams fed by dissolved N_2O inputs from groundwater. When

incorporated with riverine emissions, these findings indicate global inland water N_2O emissions of 558 (444–778) Gg N_2O yr^{-1} (Table 1). Of note, this value is higher than the estimate reported by Lauerwald et al.[1] (322 (248–590; IQR) Gg N_2O yr^{-1}), predominantly owing to the larger contribution of emissions from groundwater upwelling. However, with regard to other natural and anthropogenic sources of N_2O, inland water emissions seem to be less important. Moreover, with regard to its GWP100 (273 kg CO_2-eq. per kg N_2O), inland water N_2O emissions contribute only approximately 0.15 (0.12–0.21) Pg CO_2-eq. yr^{-1} and are thus negligible compared with CO_2 and CH_4 emissions. Overall, the GWP100 of inland water GHG emissions amounts to approximately 8.2 (6.5–10.6) Pg CO_2-eq. yr^{-1}. Net CO_2 emissions dominate the inland water GHG budget, contributing 66% (56–74%), followed by CH_4 at 32% (24–42%) and N_2O at 2% (1–3%).

Variability in emission estimates

Variability in global inland water GHG estimates reflects not only limited observations but also differences in upscaling methodology. One source of variability is the assumed water surface area[6,24], especially for headwaters and small lentic water bodies, the extent of which remains poorly constrained, although their areal emission rates are disproportionately high[25,26]. GHG emissions from lakes and reservoirs that are <0.1 km^2 can be particularly difficult to characterize robustly. Sparse observations, particularly in tropical regions and high latitudes[6,26], further limit upscaling based on regionalized estimates[9,27] or spatial interpolation[15] and instead require extrapolation using regression models[16,22], machine learning approaches[14,20] or process-based models[10–12]. More observations are needed for the smallest headwaters[25], but emissions from large lakes also remain insufficiently constrained, relying partly on statistical extrapolation and assumptions[9,15]. Similarly, current global estimates of lake CH_4 emissions do not account for the biogeochemical suppression of CH_4 production in saline lakes[28], potentially leading to overestimation of the global CH_4 flux. However, it is noteworthy that not all types of salinity suppress CH_4 formation; although salinity associated with high sulphate levels can strongly suppress CH_4 emission, carbonate salinity does not hamper CH_4 fluxes.

Further bias in existing estimates arises because many observations do not account for elevated CO_2 fluxes at night[29–31], increased CO_2 and CH_4 emissions during floods and storms[30,32], and other emission 'hot moments' that transiently amplify GHG fluxes[33–36]. Seasonality, particularly the inclusion and representation of ice cover and turnover-related emissions, also strongly affects annual budgets[37]. Pronounced spatial heterogeneity within systems, particularly for CH_4 emissions[38,39], represents another major source of uncertainty. Studies published since 2020 have partially reduced these biases through machine learning models trained to predict monthly CO_2 and CH_4 emissions[14,20]; improved annualization schemes that account for temperature, ice cover and littoral-zone contributions in lakes and reservoirs[9,22,27]; and process-based lake CH_4 models calibrated against observational time series data[11]. However, CH_4 ebullition remains particularly poorly constrained because of sparse observations and extreme spatiotemporal variability (Supplementary Table 1). For rivers, ebullition has simply been assumed to equal diffusive emissions[20]. Similarly, only one study at present has estimated global CH_4 emissions from dam release[22]. Inland water N_2O estimates[12,40–42] likewise depend on model structure, but all account for residence-time-driven N_2O reduction during denitrification and therefore yield lower values than earlier emission-factor-based estimates[6,41]. The little variability between studies of N_2O emissions is less important for the overall inland water GHG budget, given the relatively minor contribution of N_2O to total inland water GHG emissions.

Table 1 | Estimates of annual greenhouse gas fluxes by source

Gas	System	Flux estimate	Uncertainties	Refs.
CO_2	Inland waters	5.37 (3.79–7.74) Pg CO_2 yr^{-1}	5th–95th	Combination of refs. below
	Rivers	4.49 (1.65–11.56) Pg CO_2 yr^{-1}	Min–max	1
	Lakes	0.76 (0.45–1.42) Pg CO_2 yr^{-1}	Min–max	1
	Reservoirs	0.11 (0.05–0.20) Pg CO_2 yr^{-1}	Min–max	1
	Fossil fuel	34.5 (30.8–38.2) Pg CO_2 yr^{-1}	2σ	177
	Land uptake	-12.5 (-5.9 to -19.1) Pg CO_2 yr^{-1}	2σ	177
	Land use change	5.9 (0.7–10.9) Pg CO_2 yr^{-1}	2σ	177
	Ocean uptake	-9.2 (-4.8 to -13.6) Pg CO_2 yr^{-1}	2σ	177
CH_4	Inland waters	98 (78–125) Tg CH_4 yr^{-1}	5th–95th	Combination of refs. below
	Lotic	28 (17–40) Tg CH_4 yr^{-1}	5th–95th	20
	Lakes	42 (22–81) Tg CH_4 yr^{-1}	Min–max	8,9,11
	Reservoirs (from surface)	12 (10–16) Tg CH_4 yr^{-1}	Min–max	8,9,11,22
	Reservoirs (degassing)	12 (6.7–37) Tg CH_4 yr^{-1}	5th–95th	22
	Inland waters	112 (49–202) Tg CH_4 yr^{-1}	Min–max	5
	Wetlands	159 (119–203) Tg CH_4 yr^{-1}	Min–max	5
	Fossil fuel	120 (117–125) Tg CH_4 yr^{-1}	Min–max	5
	Agri + waste	211 (195–231) Tg CH_4 yr^{-1}	Min–max	5
	Ocean	12 (6–20) Tg CH_4 yr^{-1}	Min-max	5
N_2O	Inland waters	558 (444–778) Gg N_2O yr^{-1}	5th–95th	Combination of refs. below
	Streams	328 (240–415) Gg N_2O yr^{-1}	2σ	12
	Rivers	78 (73–114) Gg N_2O yr^{-1}	Min–max	12,40,41
	Lakes and reservoirs	99 (98–409) Gg N_2O yr^{-1}	Min–max	12,24,42
	Lakes	89 (46–341) Gg N_2O yr^{-1}	Min–max	12,24,42
	Reservoirs	38 (12–53) Gg N_2O yr^{-1}	Min–max	12,24,42
	Natural	~18.5 (11.5–25.0) Tg N_2O yr^{-1}	Min–max	4
	Inland and coastal waters	~0.2 (0.0–0.2) Tg N_2O yr^{-1}	Min–max	4
	Ocean	~7.4 (4.9–9.9) Tg N_2O yr^{-1}	Min–max	4
	Natural soils	~10.1 (6.1–13.5) Tg N_2O yr^{-1}	Min–max	4
	Anthropogenic	~10.2 (5.0–15.7) Tg N_2O yr^{-1}	Min–max	4
	Inland and coastal waters	~0.6 (0.2–0.8) Tg N_2O yr^{-1}	Min–max	4
	Agriculture	~5.7 (4.2–7.5) Tg N_2O yr^{-1}	Min–max	4
	Fossil fuel and industry	~1.7 (1.6–1.9) Tg N_2O yr^{-1}	Min–max	4
	Atmospheric deposition	~1.3 (1.1–1.6) Tg N_2O yr^{-1}	Min–max	4

Note that estimates from lakes and reservoirs are only for water bodies >0.1 km^2. See Supplementary Information 1 for details on methods used to produce this table.

Overall, despite progress driven by a growing body of observations and the development of new measurement and upscaling methods, quantifying inland water GHG emissions at the global scale remains challenging, although their role in the global GHG budget has been widely recognized.

Global spatial patterns and hot spots

CO_2 emissions from inland waters

As the largest contributor to global warming of the three GHGs emitted from inland waters at GWP100, CO_2 emissions exhibit distinct spatial patterns. CO_2 emission hot spots are concentrated at low latitudes (Fig. 1a), with approximately 60% of global inland water CO_2 emissions originating from regions in low latitudes (<25°). The mid-latitude (25°–50°) and high latitude (>50°) contribute equally to the remaining emissions.

The spatial distribution of inland water CO_2 emissions is primarily influenced by riverine contributions, which account for approximately 80% of total emissions despite covering only approximately 20% of the inland water surface area[1]. Approximately two-thirds of riverine CO_2 emissions originate in low latitudes, largely owing to the extensive stream surface area in these regions (approximately 50% of the global total). In addition, higher CO_2 emission rates per unit surface area further amplify emissions in low latitudes. A latitudinal gradient of declining areal river CO_2 emissions from low to high latitudes was first described in 2011[43] and later corroborated by other empirical studies[14,15].

Conversely, more than half of CO_2 emissions from lakes, including reservoirs, originate from high latitudes, which account for approximately 40% of the total lake surface area. Mid-latitude lakes contribute only one-quarter of global emissions, despite having a similar surface area to high-latitude lakes. This discrepancy reflects a higher proportion of large, deep lakes at mid-latitudes, which typically exhibit lower per-area emission rates[15,24] owing to low terrestrial carbon inputs and weaker coupling between sediment and water column processes.

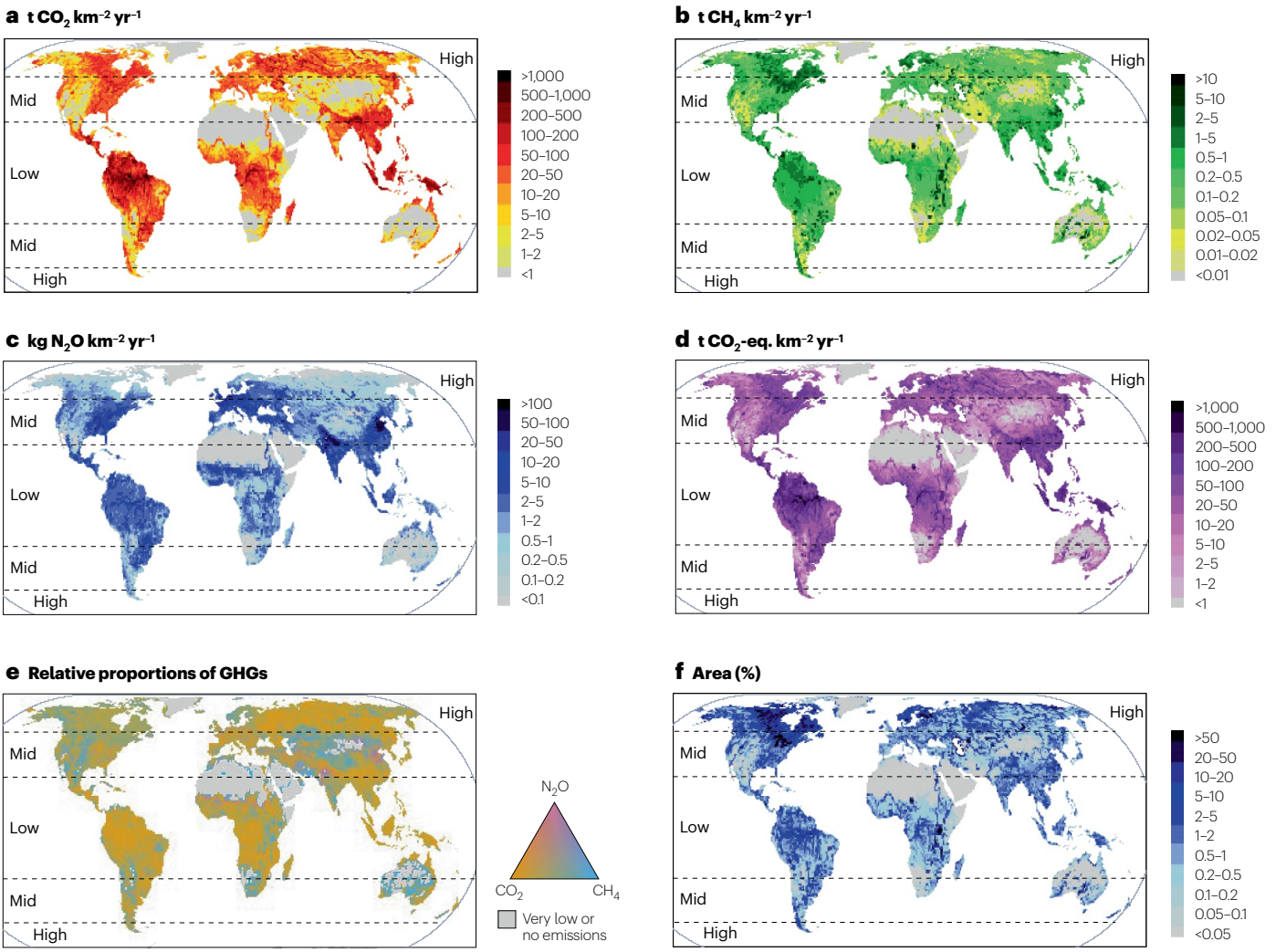

Fig. 1 | Spatial patterns of inland water GHG emissions. a–**c**, Global map of CO_2 (**a**), CH_4 (**b**) and N_2O (**c**) emissions. **d**, Combined global warming potential at a 100-year horizon (GWP100). **e**, Contribution of individual greenhouse gases (GHGs) to the GWP100. **f**, Percentage of land surface covered by inland waters, combined across streams and rivers, as well as lakes and reservoirs >0.1 km^2 in size. Bands of low latitude (<25°), mid-latitude (25°–50°) and high latitude (>50°) were used to describe global patterns in the main text.

However, emissions from very large bodies of water, such as the North American Great Lakes, which are near equilibrium with atmospheric CO_2 (refs. 44,45), are still overestimated in spatially explicit estimates because these systems are under-represented in empirical databases. Although the low latitudes exhibit the smallest lake surface area and CO_2 emissions, they show substantially higher CO_2 saturation and areal emission rates than other latitudinal bands[15,43].

The primary drivers of CO_2 emissions from inland waters are terrestrial inputs of dissolved inorganic carbon (DIC) and organic carbon[46,47]. At the global scale, these inputs are regulated by terrestrial gross primary productivity (GPP), which provides labile organic carbon for respiration in soils and inland waters, and by hydrological flows that transport carbon from soils and flooded land into inland waters. In terms of global gradients of per-area riverine CO_2 emission rates, there seems to be a saturating increase with terrestrial GPP and a non-saturating increase with runoff[16]. The tropics are a major hot spot of inland water CO_2 emissions because of both elevated terrestrial GPP and runoff. Furthermore, tropical rivers maintain strong connectivity with highly productive wetlands, which contribute substantially to CO_2 and labile organic carbon inputs[48–50].

Although inland waters are generally net heterotrophic, aquatic primary production can reduce net CO_2 emissions if autochthonous carbon is buried or exported downstream. Global-scale empirical analyses have reported a negative correlation between lake CO_2 emission rates and total phosphorus concentration (an indicator of trophic status) for large lakes[24]. Consequently, the largest global lakes are close to CO_2 equilibrium and some even serve as minor CO_2 sinks[44,45], explaining the under-representation of mid-latitude lakes in global emissions. However, substantial uncertainties remain, as systematic assessments of annual lake carbon budgets, including the seasonal interplay between aquatic productivity and CO_2 exchange, remain scarce.

A secondary control on global river CO_2 emission patterns is temperature, which influences soil and water column carbon turnover rates. Warmer temperatures accelerate carbon turnover[51], leading to higher CO_2 inputs from soils to rivers in tropical compared with high-latitude catchments[46]. Seasonal freezing of streams also notably reduces annual emissions in high-latitude and high-altitude regions[1].

CH_4 emissions from inland waters

The global spatial distribution of CH_4 emissions from inland waters is complex (Fig. 1b). For lakes (including reservoirs), low latitude (<25°), mid-latitude (25°–50°) and high latitude (>50°) each contribute approximately one-third of global CH_4 emissions. However, average per-area lake CH_4 emission rates decline substantially from low to high latitudes, with emission rates of low-latitude systems being four times higher than mid-latitude lakes and up to an order of magnitude higher than high-latitude lakes[9], a pattern also observed in reservoirs[22,52]. Despite higher average per-area emission rates from tropical systems, the larger number of lakes in more northern regions results in similar overall emissions compared with the tropics. Furthermore, limited data from large lakes (>5,000 km^2) suggest that their per-area emission rates are an order of magnitude lower than those of smaller lakes[9]. This probably reflects the tendency of larger lakes to be deeper and to have a smaller proportion of shallow littoral zones, which contribute disproportionately to overall emissions[53,54]. This size-dependent pattern, along with the prominence of large lakes in mid-latitudes, explains the spatial distribution of CH_4 emissions relative to lake surface areas. Other empirical studies have confirmed that areal CH_4 emission rates are higher in small, shallow lakes than in large, deep lakes[9,24,26]. However, the ability to map these smallest systems remains limited. Even for the very deep African Great Lakes, despite being situated at low latitudes, per-area emission rates were found to be low compared with those of smaller and shallower lakes, including those at low latitudes[21].

The decline in areal CH_4 emission rates with increasing latitude is partly attributed to the strong temperature sensitivity of CH_4 production[13,55,56]. Temperature has been used as a key predictor in multiple CH_4 emission models[9,11,22,27,57]. Additionally, empirical studies[24,58] have demonstrated substantially higher CH_4 emissions from eutrophic lakes, where elevated primary production provides labile organic carbon for methanogenesis, than from oligotrophic lakes. As a result, CH_4 emissions are notably higher in densely populated and agriculturally intensive regions of Europe, North America and Asia.

With regard to rivers, spatially resolved estimates indicate that approximately 60% of global riverine CH_4 emissions occur in low latitudes[20]. This pattern partially reflects the global distribution of river surface areas, with larger rivers in lower-latitude areas. Tropical and high-latitude streams draining organic-rich soils have been identified as CH_4 emission hot spots, driven by strong connectivity with wetland sources and, in the case of tropical systems, high rates of terrestrial productivity and soil carbon turnover[20].

When overall inland water CH_4 emissions are considered, approximately 40% of total inland water CH_4 emissions originate from low latitudes, emphasizing the role of tropical systems in global inland water GHG fluxes.

N_2O emissions from inland waters

The spatial distribution of N_2O emissions from inland water follows a distinct pattern (Fig. 1c). Most estimates have related inland water N_2O emissions to nitrogen loads[12,41,42] or nitrogen concentrations[40]. Given that N_2O emissions are largely driven by anthropogenic nitrogen pollution, emission hot spots are concentrated in densely populated and intensively farmed regions, such as Europe, East Asia, India and eastern USA[59]. Likewise, allochthonous N_2O inputs from groundwater and saturated soils, identified as an important source contributing to stream emissions, are themselves largely driven by fertilizer and manure applications. Finally, the dominance of stream emissions (Table 1), together with the major importance of nitrogen loading as an environmental driver, explains why spatial patterns in N_2O emissions are much less closely related to water surface area than is the case for CO_2 and CH_4 emissions (Fig. 1).

Approximately 50% of total N_2O emissions occur in mid-latitudes (25°–50°), with strong agreement among various estimates[12,23,40–42]. Low latitudes (<25°) contribute 38% of the global flux, largely driven by natural nitrogen loads associated with high runoff and river discharge[23,41]. By contrast, high latitudes (>50°) contribute only a small share of global N_2O emissions because both natural and anthropogenic nitrogen loads are low in these regions[12,23,40–42].

Overall inland water GHG budget

In terms of GWP100, the global warming potential of inland water GHG emissions is dominated by CO_2. Consequently, the spatial distribution of GWP100 emissions (Fig. 1d) closely mirrors that of CO_2 emissions (Fig. 1a). However, in arid regions such as the western USA, central and western Asia, Australia and southern Africa, CH_4 emissions have a larger role than CO_2 emissions, mainly owing to the predominance of lake emissions compared with riverine emissions (Fig. 1e). Overall, the global spatial pattern of inland water GWP100 emissions is therefore shaped not only by regional differences in gas composition but also,

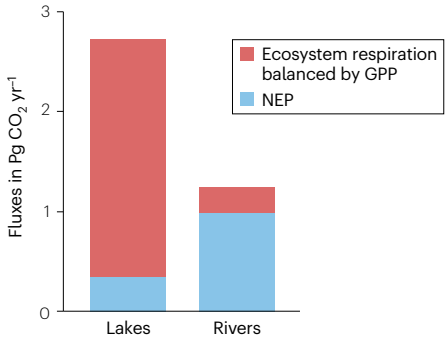

Fig. 2 | Global CO_2 budgets associated with aquatic metabolism in lakes and rivers. Data include reservoirs and are based on published syntheses[46,67]. Net ecosystem production (NEP; shown here with the sign inverted relative to the conventional definition) represents the fraction of aquatic ecosystem respiration that is not offset by aquatic gross primary production (GPP) and thus represents the net CO_2 emission sustained by aquatic metabolism.

and more fundamentally, by the distribution of inland water surface areas (Fig. 1f).

The sources and sinks of emitted GHGs

External inputs dominate inland water CO_2 emissions

On a global scale, aquatic metabolism from streams and rivers has been estimated to contribute approximately 10% of CO_2 emission fluxes[46], a value that exhibits considerable local variability, ranging from negligible to dominant[60,61]. However, that estimate was based on high global CO_2 emission totals. By comparing the global estimate of net ecosystem production (NEP; the difference between aquatic GPP and ecosystem respiration) (Fig. 2) from that study with riverine CO_2 emissions (Table 1), we estimate that aquatic metabolism accounts for approximately 20% (10–35%) of global riverine CO_2 emissions. CO_2 that is not produced within the fluvial ecosystem is transported from catchment sources (such as soil respiration) through groundwater or from fringing wetlands into streams and rivers[50]. Disentangling the CO_2 emission contributions from these various sources is not trivial and has rarely been achieved. One study found that CO_2 emissions and CO_2 from catchment sources concomitantly decreased from headwaters to larger rivers across the contiguous USA[62]. This pattern is primarily driven by a reduction in groundwater contributions to discharge — and therefore to CO_2 — downstream, with channel and valley geomorphology constraining this connectivity and its effect on CO_2 emission[63]. The pattern is further modulated by carbonate buffering, in which lotic systems with greater inputs of weathering-derived alkalinity have higher buffering capacity, which delays the downstream decline in CO_2 supersaturation[64]. Moreover, CO_2 inputs from upland groundwater discharge into streams wane downstream, whereas metabolism within the stream–river corridor (including floodplains and riparian zones) becomes dominant and increases with river size[65], marking a shift from external to internal controls on CO_2 emissions along the river continuum.

Floodplains and other fringing wetlands are other major sources of dissolved CO_2. In the central Amazon River Basin, floodplain vegetation supplies enough organic and inorganic carbon to account for the entire CO_2 emission from the river network[48]. A similarly paramount importance of wetlands sustaining high riverine CO_2 emissions was also reported for the central Congo River Basin[66]. Although the specific role of wetland vegetation and microorganisms in these carbon fluxes at the land–water interface has been conceptualized in detail[50], more quantitative information on the contribution of temporary flooded land to CO_2 emissions from streams and rivers at the global scale is needed. Filling this knowledge gap is crucial to better integrate the terrestrial and aquatic carbon budgets.

In lakes, including reservoirs, internal carbon cycling has a much larger role in CO_2 emissions than in streams and rivers. According to a global budget (that excludes the very large Caspian Sea)[67], lake GPP exceeds river GPP by an order of magnitude, although lake ecosystem respiration is approximately twice as large as that of rivers (Fig. 2). However, the NEP in lakes is only one-third of the NEP in streams and rivers. Nevertheless, with global lake (including reservoir) emissions of around 840 Tg CO_2 yr^{-1} when the Caspian Sea is excluded, approximately 40% of those emissions arise from in-lake NEP.

Dissolved organic carbon (DOC) represents the largest pool of organic carbon in the water column and feeds a large part of the CO_2 production through aquatic NEP. However, DOC is also oxidized abiotically under sunlight, and the global contribution of this process is estimated to be approximately 48–128 Tg CO_2 yr^{-1}, approximately one-tenth of the CO_2 emitted from lakes[68]. For streams and rivers, the contribution of photo-oxidation is likely lower than that in lakes owing to shorter residence times, higher turbidity and the greater effect of shading vegetation[69,70], although conclusions are more uncertain.

Most CO_2 emissions from lakes (including reservoirs) originate from allochthonous DIC. Inflows from upstream waters and groundwater are often oversaturated in CO_2, although this source is likely less substantial than for streams and rivers. Moreover, carbonate buffering partly decouples lentic DIC cycling from CO_2 emissions in both space and time, and CO_2 generated from carbonates and bicarbonates supplied from upstream contributes substantially to emissions from some systems[71], especially where carbonate precipitation occurs. Global carbonate precipitation in lakes is estimated to be 30 (10–70) Tg C yr^{-1} (ref. 72), potentially liberating 110 (37–257) Tg CO_2 yr^{-1}, given that the precipitation of one mole of carbonate releases one mole of CO_2. Although this process is likely an important source of CO_2, it remains poorly constrained by observations. Finally, a substantial amount of CO_2 emitted from some lakes has been shown to originate in the littoral zone, where lacustrine wetlands act as an atmospheric CO_2 sink but also recycle part of that CO_2 to the water column, from which it is laterally exported to the pelagic zone of lakes[73]. This process is analogous to the role of riparian wetlands in the CO_2 budgets of streams and rivers.

In summary, the aquatic ecosystem metabolism (that is, NEP), sustained by allochthonous inputs of reactive organic carbon, drives approximately one-fourth of inland water CO_2 emissions (Fig. 3a). Contributions from carbonate precipitation and photo-oxidation are minor, but these estimates come with uncertainty due to a limited number of observations. The largest portion of the emitted CO_2 seems to stem from respiration in upland soils or wetlands, but disentangling these allochthonous sources remains challenging.

Sources and sinks of inland water CH_4 emissions remain uncertain

Lakes and reservoirs are major sites of CH_4 production, with most CH_4 emissions fueled by organic matter degradation in anoxic sediments[74]. Smaller contributions come from cyanobacterial and other phytoplankton photosynthesis[75,76] in oxic surface waters and from groundwater inputs[77,78]. Both regional[79] and global studies[24,26] have reported positive relationships between CH_4 emissions and autochthonous GPP across

lakes and reservoirs. In this context, the relative role of macrophyte production in regulating CH_4 fluxes is an important area of work[80], with one study emphasizing the sizeable contribution of littoral areas to overall CH_4 outgassed in the pelagic zone of lakes[73]. In reservoirs, Arctic lakes and floodplain lakes, the role of allochthonous carbon as a substrate for methanogenesis is more pronounced because emission hot spots are frequently observed in reservoir inflow regions[39,81,82], are associated with thawing permafrost in lake sediments and along lake margins[83–86] and occur following the reflooding of extensive areas of woody and herbaceous vegetation (such as in Amazon floodplain lakes[87]). Flooded terrestrial organic matter also contributes to methane emissions from young reservoirs[88], but its contribution declines gradually with the age of the reservoir[52].

A conceptual model for how hydrology, geomorphology and land use regulate both allochthonous and autochthonous CH_4 sources in streams and rivers has been proposed[89]. Allochthonous sources — including groundwater, adjacent water saturated soils and peat deposits, and riparian wetlands — are primarily controlled by hydrology. These allochthonous CH_4 sources are important, as evidenced by strong correlations between wetland connectivity and riverine CH_4 emissions[20,66,90–92], as well as by the disproportionate contribution of headwater streams to total riverine CH_4 emissions[20,93]. A study on streams in southern Sweden showed that groundwater inputs were as important as CH_4 production in stream sediments[94]. In situ CH_4 production, which occurs mainly in benthic sediments (at the water–sediment interface), increases substantially in response to the delivery of fine sediments, organic matter and nutrients resulting from land use and land use change[89], as has been shown in both agricultural[95,96] and urban streams[97–99].

Methane oxidation removes between 45% and almost 100% of the CH_4 produced in lakes and reservoirs[74,100–102], although this process is less efficient in eutrophic systems[103]. Some evidence suggests that methane oxidation is more extensive in lakes with high phosphorus levels[104], highlighting the need for a better understanding of the balance between CH_4 production and oxidation, as well as their respective responses to warming temperatures[11,100]. In addition, methane oxidation depends on CH_4 residence time in sediments or the water column, where O_2 or other suitable electron acceptors are available[105]. Aerobic methane oxidation primarily reduces diffusive emissions and is the main microbial carbon metabolic pathway in some lakes[106]. However, most ebullitive CH_4 flux bypasses water column oxidation, except at deep sites where substantial dissolution occurs during bubble rise[107]. In rivers, methane oxidation also substantially reduces diffusive CH_4 emissions[108–110]. However, global numbers for methane oxidation have not yet been published. Although lake and reservoir models simulate these fluxes, they have only been validated against observed fluxes of CH_4 emission from the water surface[11,22].

The contribution of ebullition to methane flux varies widely, ranging from a negligible contribution in some systems to nearly 100% of emissions in other systems. On average, however, ebullition represents a substantial pathway, contributing a median of 78% and 54% of the total reservoir and lake emissions, respectively[26]. Ebullition is typically greater at the reservoirs inflows[39] and at shallower locations or areas with high sediment organic matter accumulation[80]. In a study of 349 Canadian lakes[53], nearly half of the CH_4 produced in sediments was released through ebullition. These proportions are consistent with globally up-scaled CH_4 emissions measured from the water surface of lakes[9] and reservoirs[22,27]. In reservoirs, however, an additional emission pathway — turbine outgassing — can account for approximately 55% of total CH_4 emissions[22]. Consequently, ebullition might represent only approximately 35–40% of total reservoir CH_4 emissions[22,26,27]. In rivers, ebullition contributes approximately half of total emissions[20], with the greatest degree of ebullition in shallow areas[53,54], particularly those with fine, organic rich sediments[89,111]. Despite these general patterns, however, ebullition exhibits pronounced spatiotemporal variability in both lotic[89] and lentic[112] systems making it difficult to reliably quantify this pathway at the scale of individual water bodies from point measurements. Thus, although available estimates show some convergence, ebullitive CH_4 fluxes remain highly uncertain.

Overall, based on the above estimates, ebullition and diffusion account for approximately 50% (40–54%) and 37% (29–40%) of total inland water CH_4 emissions, respectively (Fig. 3b). Outgassing from dams contributes the remaining 13% (7–31%) of the assessed emission flux. Additional pathways, such as emissions through emergent

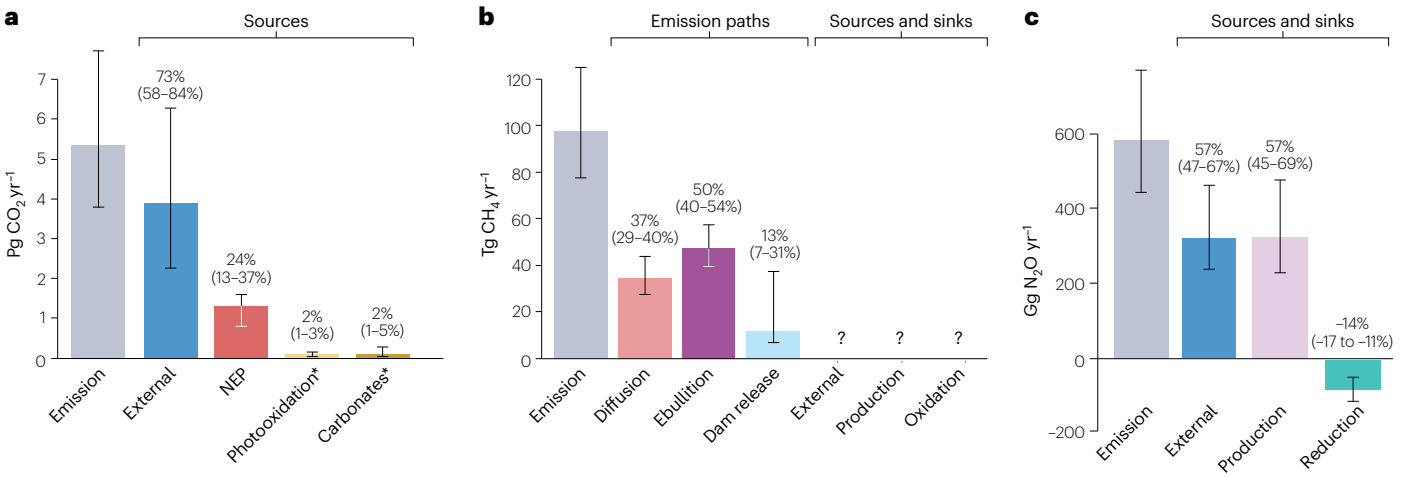

Fig. 3 | Greenhouse gas budgets of the global inland water network. a, CO_2 budget. **b**, CH_4 budget. **c**, N_2O budget. Whiskers represent the 5th–95th percentile uncertainty ranges. Percentages refer to the share of each component relative to total emissions. In **a**, the asterisk indicates that photochemical oxidation and carbonate precipitation fluxes are shown only for lakes and reservoirs; in rivers, these pathways are expected to be even less important contributors to GHG emissions. In **b**, question marks denote flux components that remain unquantified. NEP, net ecosystem production.

vegetation, have not yet been quantified at the global scale. Likewise, key internal processes, including global production and oxidation of CH_4 within inland waters, as well as allochthonous CH_4 inputs, remain poorly constrained and largely unknown.

External inputs are a substantial source of inland water N_2O emissions

Inland water nitrous oxide (N_2O) is primarily produced as a by-product of nitrification and as an intermediate of denitrification. Nitrification involves the oxidation of ammonium (NH_4^+) to nitrate (NO_3^-) under oxic conditions, producing N_2O as a by-product. NH_4^+ is derived from organic matter mineralization and accumulates under anoxic conditions, where nitrification is inhibited. Hot spots of N_2O production arise where NH_4^+-rich anoxic waters meet oxygenated waters, such as groundwater–surface water interfaces or metalimnia (the transition zone between anoxic bottom waters and oxygenated surface waters in lakes), and during lake turnover events[6].

Denitrification reduces NO_3^- to N_2O and ultimately to dinitrogen (N_2) under anoxic conditions. Whether N_2O accumulates or is further reduced to N_2 depends on environmental factors. For example, low nitrate and long residence times favour complete reduction to N_2, whereas high nitrate and low organic carbon tend to increase N_2O yields[6]. Denitrification occurs in water-saturated soils, groundwater, benthic sediments and hypolimnetic waters of stratified lakes.

In streams and rivers, only a minority of emitted N_2O is produced within the water column, with global modelling studies estimating this contribution to be approximately 14–18%[23,113]. Instead, streambed sediments and inputs from saturated soils and groundwater are typically more important sources of N_2O, especially in headwaters, which contribute disproportionately to fluvial N_2O emissions[23,40,114]. Estimates of the amount of N_2O consumed by denitrification within streams and rivers are scarce; to our knowledge, only one modelling study exists, which estimated that 20% of total global riverine N_2O is further reduced to N_2 (ref. 23).

Process-based models of inland water nitrogen cycling often primarily attribute external or benthic sources of N_2O to denitrification under low oxygen conditions[23,113]. However, nitrification is the dominant mode of N_2O production in water-saturated riparian soils, which then becomes a substantial N_2O source to streams and rivers[115,116]. Despite this observation, many empirical syntheses still find denitrification to be the prevailing factor determining stream and river N_2O emissions across different climate zones and environmental settings[40,117]. Similarly, riparian denitrification was identified as an important N_2O source to large tropical river networks during flooding[118].

In lakes and reservoirs, reactive nitrogen input from rivers and groundwater is the major source of N_2O production[12,119]. Converging evidence from process-based modelling[42,113] and empirical studies[120,121] indicates that nitrification in oxygenated waters and littoral sediments is often the primary source of emitted N_2O. Denitrification in anoxic hypolimnia or sediments also produces N_2O, but when nitrate becomes limiting, N_2O is often further reduced to N_2, lowering net N_2O emissions[120,121]. Indeed, approximately half of the N_2O produced internally in lakes and reservoirs is consumed by denitrification before reaching the atmosphere[41,42].

At the scale of the entire inland water network, groundwater and water-saturated riparian soils are major sources of N_2O. One estimate[113] indicated that these inputs account for approximately 47% of total N_2O emissions, whereas earlier estimates[122] suggested that approximately two-thirds of inland water N_2O emissions originate from groundwater sources. We consider these two estimates as lower and upper bounds of the allochthonous N_2O contribution (Fig. 3c). Finally, taking into account the above data, we estimate that denitrification removes approximately one-quarter of the N_2O produced within inland waters (Supplementary Table 1). However, this flux remains highly uncertain, and the scarcity of quantitative estimates precludes the ability to define a reliable uncertainty range.

Evolution of emissions under global change

Anthropogenic perturbations have increased inland water GHG emissions and are expected to continue doing so throughout the twenty-first century. These perturbations include direct effects such as eutrophication and river damming, as well as indirect effects mediated by climate change and global greening driven by rising atmospheric CO_2 concentrations and warming temperatures. However, the extent of these perturbations and the dominant anthropogenic drivers involved differ substantially among inland water emissions of CO_2, CH_4 and N_2O (Supplementary Fig. 1).

Drivers of long-term emission trends

Climate change and global greening enhance inland water CO_2 emissions. Inland water CO_2 budgets are largely controlled by terrestrial inputs of DIC and labile organic carbon from surrounding ecosystems, with their effects modulated by water residence time and system chemistry[123]. These inputs scale with both terrestrial primary production and hydrological transfer efficiency, such as runoff and wetland connectivity. Empirical syntheses have identified terrestrial productivity as a strong predictor of spatial CO_2 emission patterns[14,16,124,125], a link further supported by isotopic tracer experiments[126]. Process-based reconstructions and projections likewise primarily attribute historical and future emission increases to enhanced productivity driven by CO_2 fertilization, climate and land use[10,127,128]. Soil carbon losses also contribute to inland water CO_2 emissions, as agricultural erosion mobilizes particulate organic carbon (POC) from soils. However, fluvial transport of soil-derived POC occurs primarily during high-flow events; when flows are lower, erosion mobilizes far less POC, and any suspended POC is likely to settle out through sedimentation. Accordingly, soil derived POC undergoes less decomposition in transit as leached DOC[128]. By contrast, permafrost thaw releases old yet often labile organic matter that fuels aquatic CO_2 emissions[129]. Warming further enhances these emissions by accelerating decomposition both on land and in waters[130].

In lotic inland waters, discharge and floodplain connectivity regulate the delivery of dissolved carbon from soils and wetlands and thus control CO_2 emissions[14,92,131]. Engineering structures that sever river–floodplain connectivity, such as levees, can reduce CO_2 emissions from the river channel itself[132]. However, the associated degradation of floodplain ecosystems potentially reduces their ability to sequester atmospheric CO_2 (ref. 133). Flowpaths are as important as flow volumes; in permafrost regions, thaw-induced deepening of drainage and increasing groundwater contributions enhance soil-respired CO_2 delivery to rivers[134,135]. Similarly, higher precipitation in boreal regions has been found to induce shallower flowpaths and inflows with diluted CO_2 concentrations, leading to lower CO_2 evasion from lakes[125,136].

In lentic systems with low allochthonous inputs, such as some large lakes, eutrophication-driven production can reduce net heterotrophy and suppress CO_2 emissions[24]. At the network scale, the combined effects of damming and eutrophication have been shown to reduce CO_2 evasion in some settings[137]. However, much of the newly produced

autochthonous organic carbon is eventually remineralized in the water column or sediments. Quantifying the net effect of eutrophication on inland water CO_2 budgets requires integrated analyses of whole inland water networks that account for seasonal dynamics and advective transport.

Warming, eutrophication and damming enhance inland water CH_4 emissions. Warming is a major control on CH_4 emissions. Meta-analyses have demonstrated a strong temperature sensitivity of CH_4 emissions across a range of aquatic ecosystems[56]. Observed latitudinal gradients[13] and long-term warming experiments[95] corroborate this temperature sensitivity. However, temperature effects are substrate limited. For example, despite their warm climate, the African Great Lakes remain low CH_4 emitters because of only modest inputs of nutrients and organic matter[21]. In rivers, a global analysis of spatial patterns in diffusive emissions and its environmental drivers[20] did not identify temperature as an important control, potentially reflecting the relatively limited importance of in situ production, and hence of its temperature sensitivity, for diffusive emissions. In addition, both in situ CH_4 production and CH_4 oxidation can increase with the temperature of the water column and benthic sediments, weakening the net relationship between temperature and diffusive emissions. By contrast, riverine CH_4 emissions through ebullition, estimated to contribute half of river CH_4 emissions[20], are expected to be highly temperature sensitive[138]. Given the importance of inland waters as a source of atmospheric CH_4, the temperature sensitivity of CH_4 production and emissions constitutes a potentially important positive climate feedback.

In lakes and reservoirs, CH_4 emissions rise with trophic state. Greater productivity increases the supply of labile organic matter that fuels methanogenesis[24,139], a relationship used to inform space-for-time projections of future emissions[140]. The bathymetric shape of the system strongly influences these emissions in both lakes and reservoirs, with large littoral zones delivering more sedimentary CH_4 to the epilimnetic waters, from which it can be released to the atmosphere[53,57]. However, chemical constraints can offset these effects. For example, salinization resulting from drought, irrigation return flows or sea-level rise can suppress methanogenesis[28]. Long-term CH_4 trajectories therefore depend on the balance between processes that stimulate organic matter production and those that inhibit methane production.

Hydrology regulates residence time, stratification and anoxia, all of which are key controls for CH_4 production and release, including ebullition. Global lake surface area has expanded by approximately 46,000 km^2 (approximately 1.6 %) since 2000, with approximately half of that area contributed by new reservoirs[141]. Reservoirs are a major anthropogenic CH_4 source[139,142] for two main reasons. First, flooding of biomass and soils yields post-impoundment CH_4 pulses[88] and, second, the degassing of anoxic, CH_4-rich hypolimnetic waters through turbines and spillways can contribute emissions comparable to surface fluxes[22]. Pre-clearing of terrestrial biomass and soils before inundation reduces, but does not eliminate, this signal; site selection and operation thus strongly shape net emissions[143]. Moreover, the progressive depletion of labile carbon in flooded soils tends to reduce CH_4 production and emissions over time, such that reservoir age becomes an important control on emission rates[52,144].

In many regions, eutrophication, warming and river damming interact synergistically to increase inland water CH_4 emissions. Permafrost thaw can further amplify emissions by creating or expanding thermokarst lakes, which are often CH_4 hot spots dominated by ebullition[86,145–147]. Increased ebullition also occurs in low-order streams within thawing catchments[148]. However, permafrost thaw does not always expand water surface area[149] and, in some regions, leads to declines in water surface area[150]. As warming accelerates permafrost degradation, a better understanding of the projected effects on lake formation, expansion and drainage is needed to constrain the CH_4 contribution from high-latitude waters. Nevertheless, a warming climate is expected to have a greater relative effect on methane emissions from high-latitude lakes than on those from lower latitudes because of both temperature effects and the prolonging of ice-free seasons[13].

Eutrophication enhances inland water N_2O emissions. The dominant long-term driver of N_2O emissions is reactive nitrogen inputs to groundwater and surface water, as shown by both empirical and process-based modelling studies. Process-based models, in particular, have identified that agricultural runoff from excessive fertilizer and manure applications is the main cause of rising N_2O emissions from both lentic and lotic inland waters[12,23,113]. Reports of eutrophic farm ponds in Canada acting as N_2O sinks[151] probably reflect summer-only sampling; boreal lakes show strong seasonality with winter peaks, implying that summer-based estimates might underestimate annual fluxes[152].

Temperature accelerates nitrification and denitrification, but temperature effects on net N_2O flux depend on the N_2O to N_2 product ratio. One meta-analysis indicated that warming generally increases inland water denitrification and N_2O emissions, albeit with strong variation across climates, environmental gradients and study methodology[153]. Conversely, findings from a 2-year field study of a temperate, urbanized stream using stable isotopes suggest that higher temperatures promote more complete denitrification (lower N_2O to N_2 ratio), thereby reducing N_2O emissions under certain conditions[154]. In addition, empirical work on boreal lakes has shown elevated N_2O emissions during the cold season, driven by enhanced denitrification following nitrate accumulation associated with reduced terrestrial and aquatic productivity, and further amplified by less complete denitrification under high nitrate availability[152]. Under such conditions, climate warming could reduce cold-season N_2O emissions by lengthening the growing season and increasing terrestrial and aquatic productivity, thereby enhancing nitrate uptake by vegetation. Overall, temperature effects on inland water N_2O emissions are strongly context dependent and mediated by oxygen, nitrate and carbon supply, productivity, and residence time.

Hydrological regulation is also an important determinant of N_2O emissions. River damming lengthens residence times and promotes anoxia, potentially increasing denitrification and N_2O production within inland waters. However, basin-scale consequences remain uncertain, partly because in-river increases in N_2O production can be partially offset by reduced denitrification in downstream floodplains and coastal ecosystems[155]. Moreover, denitrification under increased residence time can lead to N_2O reduction and thus does not necessarily lead to increased emissions. A global modelling study[12] concluded that damming has made only a limited contribution to historical increases in N_2O compared with the dominant effect of rising river nitrogen loads.

The magnitude of anthropogenic perturbations

For CO_2, early work suggested that more than half of inland water CO_2 emissions could be anthropogenic[156]. Global studies using a data-ensemble method[18] and an integrated modelling approach[10] later estimated that approximately a quarter of inland water CO_2 emissions are anthropogenic, largely because of proportionally increased

terrestrial carbon input. The dominant drivers are land use change and climate-driven increases in carbon mobilization through altered hydrology, with additional indirect effects from CO_2 fertilization and nitrogen enrichment (such as from fertilizer, manure and atmospheric deposition), which stimulate terrestrial primary production and thereby carbon delivery to aquatic systems[10].

For CH_4, a global budget[5] published in 2025 provided a first-order estimate that approximately 50% of inland water CH_4 emissions originate from anthropogenic perturbations, including river damming and eutrophication. Of this anthropogenic component, 4% and 22% of emissions were estimated to come directly from human-created farm ponds and reservoirs, and the remaining 23% were attributed to eutrophication-related increases in emissions from lakes, ponds, rivers and streams[5]. A single integrated framework that simultaneously represents all these drivers across all inland water types is not yet available.

The anthropogenic signal is clearest for N_2O because inland water nitrogen loads are strongly influenced by human activities — primarily mineral fertilizer use, but also manure and wastewater inputs. Global modelling indicates that approximately 65–70% of inland water N_2O emissions are anthropogenic[12,113], consistent with the latest IPCC assessment and global N_2O budgets[4,157].

Expressed as CO_2 equivalents (GWP100), the combined direct and indirect effects of anthropogenic perturbations since the pre-Industrial period have increased inland water GHG emissions by approximately 2.8 (2.3–3.5) Pg CO_2-eq. yr^{-1} (Supplementary Information 1). This increase is equal to approximately one-third of total inland water GHG emissions. CO_2 and CH_4 each contribute roughly half of the anthropogenic perturbation (Fig. 4a), whereas N_2O contributes only approximately 4% of the anthropogenic CO_2-eq. total, owing to its smaller absolute flux. By contrast, natural inland water GHG emissions are dominated by CO_2, which accounts for about three-quarters of the total. Most of the remaining emissions are attributable to CH_4, whereas N_2O contributes only approximately 1% of natural inland water GHG emissions (Fig. 4b).

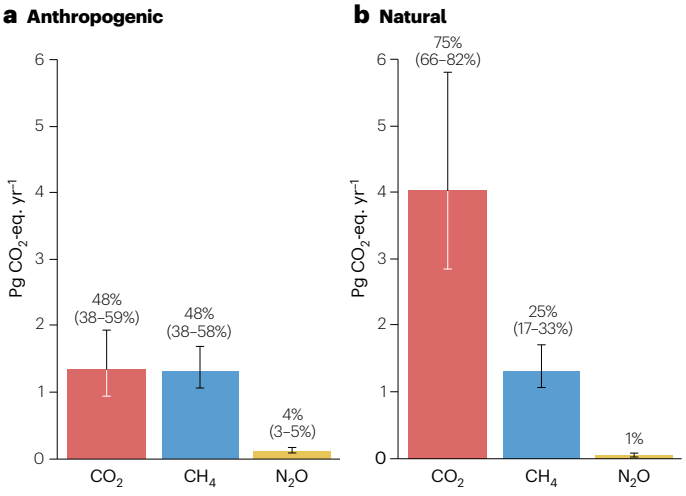

Fig. 4 | Natural and anthropogenic contributions to inland water GHG emissions. a,**b**, Partitioning of inland water GHG budgets into (**a**) anthropogenic and (**b**) natural components. Whiskers indicate 5th–95th percentile uncertainty ranges. Percentages denote the contribution of each component relative to the total natural or anthropogenic share of inland water GHG emissions. Refer to Supplementary Information 1 for methods.

Globally, the rise in inland water CO_2 emissions is primarily driven by indirect anthropogenic effects that parallel broader human-induced disruption to the land carbon budget, which includes terrestrial ecosystems, wetlands and inland waters. Taking a net land CO_2 uptake of 6.6 Pg CO_2 yr^{-1} (ref. 157) as a reference, the anthropogenic enhancement of inland water CO_2 emissions probably offsets roughly 10–25% of the terrestrial carbon sink, assuming that these excess aquatic emissions would otherwise have contributed to land carbon storage. Relative to the magnitude of the total anthropogenic inland water GHG perturbation, the resulting excess emissions offset close to one-third of the land carbon sink.

By contrast, current anthropogenic N_2O and CH_4 emissions from inland waters are more directly linked to human activities such as river damming and eutrophication. Accordingly, mitigation efforts could prioritize reservoir management and reductions in nutrient loads through improved wastewater treatment and sustainable land use and fertilization practices. On the basis of the GHG budgets of the Global Carbon Project[4,5], inland waters account for approximately 15% of anthropogenic CH_4 emissions[5], whereas their contribution to anthropogenic N_2O probably does not exceed approximately 5%[4] when excluding coastal waters and natural wetlands. These results underscore that inland water GHG emissions can no longer be treated as purely natural and highlight the need to explicitly distinguish between anthropogenic and natural components in global GHG budgets.

Future trends of GHG emissions

Integrated, process-based models have reconstructed historical responses of inland water CO_2 and N_2O emissions to climate, land use, river damming and wastewater management[10,12,113]. However, global forward projections for these gases remain largely absent.

Because tropical rivers dominate global inland water CO_2 emissions, they strongly influence future global emission trajectories. Basin-scale modelling studies project twenty-first-century increases in emissions from the Amazon and Congo River Basins, driven by greater terrestrial carbon inputs linked to rising primary production — and, in the case of the Congo River Basin, by increased runoff[127,158]. However, other studies indicate that future productivity gains will be more limited in the tropics and instead shift towards temperate–boreal regions[159,160]. In addition, streamflow is projected to increase in tropical Africa and Asia and across boreal to Arctic basins, with little change in the Amazon River Basin[161]. These projections for the Amazon River Basin contrast with recent observations of increasing floodplain inundation in the central Amazon River Basin[162], which probably enhances the delivery of CO_2 and labile organic carbon to the river network. For Arctic basins, these trends are already emerging[163]. By contrast, future dam construction has the potential to reduce inland water CO_2 emissions by decreasing net heterotrophy within aquatic networks and by weakening floodplain–river connectivity downstream. However, the net effect of future dam expansion on inland water CO_2 emissions remains difficult to quantify without a fully integrated modelling framework but is likely smaller than the effects of changes in runoff and terrestrial primary productivity. Notably, the current rise in dam construction is concentrated in the global south, including tropical river systems such as the Mekong River Basin[164], and growing demand for irrigation and hydropower is projected for Europe, South Asia and Africa[165]. Together, increased inland water CO_2 emissions seem most plausible for tropical Africa, Southeast Asia, and boreal to Arctic regions, with the latter contributing less to the global total.

Several projections for CH_4 emissions exist. One study that accounted for changes in temperature and ice coverage, regional variations in surface water extent and phosphorus levels, and planned dam construction estimated that global lake and reservoir CH_4 emissions could increase by 24–91% by 2080–2099[13]. Another study projected an approximately 10–45% increase in reservoir CH_4 emission based on planned dam construction[52], although that estimate did not consider eutrophication and warming effects. Importantly, the future trajectory of eutrophication is not well known, with some regional[166] and global[167] studies indicating no clear increase. Assuming strong eutrophication, an approximately 30–90% increase in CH_4 emissions from lakes and reservoirs has been projected with a twofold to threefold rise in phosphorus concentrations[140,168]. Of note, however, these phosphorus scenarios are likely too high; a comprehensive impact model projected that phosphorus delivery to inland waters will increase by up to 24% by 2050 and 40% by 2070[59]. Moreover, phosphorus increases in natural lakes are expected to be smaller than in reservoirs, as many are remote and weakly connected to nutrient-rich river networks[169]. Current projections also do not account for trends in water salinization because of sea level rise, climate change or irrigation water use. Because future perturbations related to dam construction[164], eutrophication[59] and soil losses[170] to inland waters are expected to be concentrated mainly in the global south, their synergistic interactions have the potential to drive particularly strong increases in inland water CH_4 emissions in these regions.

For N_2O, an empirical global projection estimated increases of up to 35% (2000–2050), driven by 47% increases in riverine dissolved inorganic N loads[171], broadly consistent with other N-load scenarios[59]. Although there is broad consensus that inland water emissions of all three GHGs will increase over the twenty-first century, robust end-century global projections, which would account for all of the main environmental drivers, are still missing, highlighting a key gap that could be addressed in future studies.

Summary and future perspectives

Inland waters occupy only a small fraction of Earth's surface, yet they represent a major source of GHGs to the atmosphere (approximately 8.2 (6.5–10.6) Pg CO_2-eq. yr^{-1} GWP100). Emissions are dominated by CO_2, with smaller contributions from CH_4, and N_2O accounting for only a minor share. More than half of emissions arise from below 25° latitude. A substantial fraction of emissions is sustained by allochthonous inputs from groundwater, as well as adjacent soils and wetlands. With regard to the drivers of GHG emissions, direct and indirect anthropogenic perturbations since the Industrial Revolution have increased inland water GHG emissions by approximately 2.8 (2.3–3.5) Pg CO_2-eq. yr^{-1}, which presents approximately one-third of present-day emissions. Emissions are likely to rise further over the twenty-first century, particularly in the global south because of damming, eutrophication and soil losses to inland waters, and at high latitudes owing to permafrost thaw, increasing runoff and enhanced terrestrial productivity. However, it is important to note that estimates of inland water emissions remain highly uncertain because observations are sparse, especially in tropical and high-latitude regions, and because spatiotemporal variability remains poorly captured.

Improving estimates of present-day inland water GHG emissions requires more multi-year, high-frequency observations that resolve diel, seasonal and interannual variability across a wide range of inland water types. Such studies should systematically capture internal spatial heterogeneity along gradients of depth, sediment properties and allochthonous influence within individual water bodies and networks. The development of cost-effective automated sensors on fixed[172,173], floating[174] and drone-based[175,176] platforms is particularly promising for strengthening the observational basis needed for upscaling, as well as for calibrating and validating process-based models.

Process-based models demonstrate strong potential for capturing diel, seasonal and interannual variability in inland water GHG emissions. In particular, integrating the coupled GHG dynamics of terrestrial ecosystems, wetlands and inland waters within land surface models could provide a more consistent assessment of their combined budgets and anthropogenic perturbations while avoiding double counting and gaps. A major remaining challenge is the inclusion of very small water bodies, such as ponds and ditches, which are likely important but poorly constrained GHG sources and remain difficult to map even at a regional scale.

Increases in inland water GHG emissions driven by rising atmospheric CO_2 and climate change largely represent a positive feedback to global climate change. By contrast, reducing eutrophication and soil losses to inland waters offers a direct mitigation opportunity, particularly for developing countries within the global south, where land use expansion and river damming continue to increase and where high temperatures further enhance GHG production. Moreover, explicitly accounting for the expected lifetime of GHG emissions in future modelling studies could help to increase understanding of GHG emissions associated with new reservoirs.

Published online: 30 September 2026

References

1. Lauerwald, R. et al. Inland water greenhouse gas budgets for RECCAP2: 2. Regionalization and homogenization of estimates. *Glob. Biogeochem. Cycles* **37**, e2022GB007658 (2023).
2. Friedlingstein, P. et al. Global carbon budget 2024. *Earth Syst. Sci. Data* **17**, 965–1039 (2025).
3. Cole, J. J. et al. Plumbing the global carbon cycle: integrating inland waters into the terrestrial carbon budget. *Ecosystems* **10**, 172–185 (2007).
4. Tian, H. et al. Global nitrous oxide budget (1980–2020). *Earth Syst. Sci. Data* **16**, 2543–2604 (2024).
5. Saunois, M. et al. Global methane budget 2000–2020. *Earth Syst. Sci. Data* **17**, 1873–1958 (2025).
6. Lauerwald, R. et al. Inland water greenhouse gas budgets for RECCAP2: 1. State-of-the-art of global scale assessments. *Glob. Biogeochem. Cycles* **37**, e2022GB007657 (2023).
7. Zscheischler, J. et al. Reviews and syntheses: an empirical spatiotemporal description of the global surface–atmosphere carbon fluxes: opportunities and data limitations. *Biogeosciences* **14**, 3685–3703 (2017).
8. Stavert, A. R. et al. Regional trends and drivers of the global methane budget. *Glob. Change Biol.* **28**, 182–200 (2022).
9. Johnson, M. S., Matthews, E., Du, J., Genovese, V. & Bastviken, D. Methane emission from global lakes: new spatiotemporal data and observation-driven modeling of methane dynamics indicates lower emissions. *J. Geophys. Res.* **127**, e2022JG006793 (2022).
10. Tian, H. et al. Increased terrestrial carbon export and CO_2 evasion from global inland waters since the preindustrial era. *Glob. Biogeochem. Cycles* **37**, e2023GB007776 (2023).
11. Zhuang, Q. et al. Current and future global lake methane emissions: a process-based modeling analysis. *J. Geophys. Res.* **128**, e2022JG007137 (2023).
12. Li, Y. et al. Increased nitrous oxide emissions from global lakes and reservoirs since the pre-industrial era. *Nat. Commun.* **15**, 942 (2024).
13. Bastviken, D. & Johnson, M. S. Future methane emissions from lakes and reservoirs. *Nat. Water* https://doi.org/10.1038/s44221-025-00532-6 (2025).
14. Liu, S. et al. The importance of hydrology in routing terrestrial carbon to the atmosphere via global streams and rivers. *Proc. Natl Acad. Sci. USA* **119**, e2106322119 (2022).
15. Raymond, P. A. et al. Global carbon dioxide emissions from inland waters. *Nature* **503**, 355–359 (2013).
16. Lauerwald, R., Laruelle, G. G., Hartmann, J., Ciais, P. & Regnier, P. A. G. Spatial patterns in CO_2 evasion from the global river network. *Glob. Biogeochem. Cycles* **29**, 534–554 (2015).
17. Abril, G. et al. Technical note: large overestimation of pCO_2 calculated from pH and alkalinity in acidic, organic-rich freshwaters. *Biogeosciences* **12**, 67–78 (2015).
18. Regnier, P., Resplandy, L., Najjar, R. G. & Ciais, P. The land-to-ocean loops of the global carbon cycle. *Nature* **603**, 401–410 (2022).

19. Ciais, P. et al. Definitions and methods to estimate regional land carbon fluxes for the second phase of the REgional Carbon Cycle Assessment and Processes Project (RECCAP-2). *Geosci. Model Dev.* **15**, 1289–1316 (2022).
20. Rocher-Ros, G. et al. Global methane emissions from rivers and streams. *Nature* **621**, 530–535 (2023).
21. Borges, A. V. et al. Greenhouse gas emissions from African lakes are no longer a blind spot. *Sci. Adv.* **8**, eabi8716 (2022).
22. Harrison, J. A., Prairie, Y. T., Mercier-Blais, S. & Soued, C. Year-2020 global distribution and pathways of reservoir methane and carbon dioxide emissions according to the greenhouse gas from reservoirs (G-res) model. *Glob. Biogeochem. Cycles* **35**, e2020GB006888 (2021).
23. Yao, Y. et al. Increased global nitrous oxide emissions from streams and rivers in the Anthropocene. *Nat. Clim. Change* **10**, 138–142 (2020).
24. DelSontro, T., Beaulieu, J. J. & Downing, J. A. Greenhouse gas emissions from lakes and impoundments: upscaling in the face of global change. *Limnol. Oceanogr. Lett.* **3**, 64–75 (2018).
25. Marx, A. et al. A review of CO_2 and associated carbon dynamics in headwater streams: a global perspective. *Rev. Geophys.* **55**, 560–585 (2017).
26. Deemer, B. R. & Holgerson, M. A. Drivers of methane flux differ between lakes and reservoirs, complicating global upscaling efforts. *J. Geophys. Res.* **126**, e2019JG005600 (2021).
27. Johnson, M. S. et al. Spatiotemporal methane emission from global reservoirs. *J. Geophys. Res.* **126**, e2021JG006305 (2021).
28. Soued, C. et al. Salinity causes widespread restriction of methane emissions from small inland waters. *Nat. Commun.* **15**, 717 (2024).
29. Gómez-Gener, L. et al. Global carbon dioxide efflux from rivers enhanced by high nocturnal emissions. *Nat. Geosci.* **14**, 289–294 (2021).
30. Woodrow, R. L. et al. Enhanced stream greenhouse gas emissions at night and during flood events. *Limnol. Oceanogr. Lett.* **9**, 276–285 (2024).
31. De Eyto, E. et al. Diel variation in CO_2 flux is substantial in many lakes. *Limnol. Oceanogr. Lett.* **10**, 977–989 (2025).
32. Almeida, R. M., Pacheco, F. S., Barros, N., Rosi, E. & Roland, F. Extreme floods increase CO_2 outgassing from a large Amazonian river. *Limnol. Oceanogr.* **62**, 989–999 (2017).
33. Harrison, J. A., Deemer, B. R., Birchfield, M. K. & O'Malley, M. T. Reservoir water-level drawdowns accelerate and amplify methane emission. *Environ. Sci. Technol.* **51**, 1267–1277 (2017).
34. Denfeld, B. A., Baulch, H. M., Del Giorgio, P. A., Hampton, S. E. & Karlsson, J. A synthesis of carbon dioxide and methane dynamics during the ice-covered period of northern lakes. *Limnol. Oceanogr. Lett.* **3**, 117–131 (2018).
35. Mayr, M. J., Zimmermann, M., Dey, J., Wehrli, B. & Bürgmann, H. Lake mixing regime selects apparent methane oxidation kinetics of the methanotroph assemblage. *Biogeosciences* **17**, 4247–4259 (2020).
36. López-Rojo, N. et al. Carbon emissions from inland waters may be underestimated: evidence from European river networks fragmented by drying. *Limnol. Oceanogr. Lett.* **9**, 553–562 (2024).
37. Rosentreter, J. A. et al. Half of global methane emissions come from highly variable aquatic ecosystem sources. *Nat. Geosci.* **14**, 225–230 (2021).
38. Colas, F. et al. Spatial and temporal variability of diffusive CO_2 and CH_4 fluxes from the Amazonian reservoir Petit-Saut (French Guiana) reveals the importance of allochthonous inputs for long-term C emissions. *Glob. Biogeochem. Cycles* **34**, e2020GB006602 (2020).
39. Linkhorst, A. et al. Spatially resolved measurements in tropical reservoirs reveal elevated methane ebullition at river inflows and at high productivity. *Glob. Biogeochem. Cycles* **35**, e2020GB006717 (2021).
40. Marzadri, A. et al. Global riverine nitrous oxide emissions: the role of small streams and large rivers. *Sci. Total Environ.* **776**, 145148 (2021).
41. Maavara, T. et al. Nitrous oxide emissions from inland waters: are IPCC estimates too high? *Glob. Change Biol.* **25**, 473–488 (2019).
42. Lauerwald, R. et al. Natural lakes are a minor global source of N_2O to the atmosphere. *Glob. Biogeochem. Cycles* **33**, 1564–1581 (2019).
43. Aufdenkampe, A. K. et al. Riverine coupling of biogeochemical cycles between land, oceans, and atmosphere. *Front. Ecol. Environ.* **9**, 53–60 (2011).
44. Karim, A., Dubois, K. & Veizer, J. Carbon and oxygen dynamics in the Laurentian Great Lakes: implications for the CO2 flux from terrestrial aquatic systems to the atmosphere. *Chem. Geol.* **281**, 133–141 (2011).
45. Sandborn, D. E. & Minor, E. C. Underway pCO_2 surveys unravel CO_2 invasion of lake superior from seasonal variability. *J. Geophys. Res.* **129**, e2023JG007877 (2024).
46. Battin, T. J. et al. River ecosystem metabolism and carbon biogeochemistry in a changing world. *Nature* **613**, 449–459 (2023).
47. Tranvik, L. J. et al. Lakes and reservoirs as regulators of carbon cycling and climate. *Limnol. Oceanogr.* **54**, 2298–2314 (2009).
48. Abril, G. et al. Amazon River carbon dioxide outgassing fuelled by wetlands. *Nature* **505**, 395–398 (2014).
49. Duvert, C. et al. Hydroclimate and landscape diversity drive highly variable greenhouse gas emissions from tropical and subtropical inland waters. *Nat. Water* **3**, 1303–1317 (2025).
50. Abril, G. & Borges, A. V. Ideas and perspectives: carbon leaks from flooded land: do we need to replumb the inland water active pipe? *Biogeosciences* **16**, 769–784 (2019).
51. Raich, J. W. & Schlesinger, W. H. The global carbon dioxide flux in soil respiration and its relationship to vegetation and climate. *Tellus B* **44**, 81 (1992).
52. Soued, C., Harrison, J. A., Mercier-Blais, S. & Prairie, Y. T. Reservoir CO2 and CH4 emissions and their climate impact over the period 1900–2060. *Nat. Geosci.* **15**, 700–705 (2022).
53. Kim, J., Thottathil, S. D. & Prairie, Y. T. A simple approach to quantifying whole-lake methane ebullition and sedimentary methane production, and its application to the Canadian Lake Pulse dataset. *Limnol. Oceanogr.* **70**, 393–410 (2025).
54. Langenegger, T., Vachon, D., Donis, D. & McGinnis, D. F. What the bubble knows: lake methane dynamics revealed by sediment gas bubble composition. *Limnol. Oceanogr.* **64**, 1526–1544 (2019).
55. Aben, R. C. H. et al. Cross continental increase in methane ebullition under climate change. *Nat. Commun.* **8**, 1682 (2017).
56. Yvon-Durocher, G. et al. Methane fluxes show consistent temperature dependence across microbial to ecosystem scales. *Nature* **507**, 488–491 (2014).
57. Prairie, Y. T. et al. A new modelling framework to assess biogenic GHG emissions from reservoirs: the G-res tool. *Environ. Model. Softw.* **143**, 105117 (2021).
58. Rinta, P. et al. Higher late summer methane emission from central than northern European lakes. *J. Limnol.* https://doi.org/10.4081/jlimnol.2016.1475 (2016).
59. Beusen, A. H. W. et al. Exploring river nitrogen and phosphorus loading and export to global coastal waters in the shared socio-economic pathways. *Glob. Environ. Change* **72**, 102426 (2022).
60. Solano, V. et al. Stream respiration exceeds CO_2 evasion in a low-energy, oligotrophic tropical stream. *Limnol. Oceanogr.* **68**, 1132–1146 (2023).
61. Diamond, J. S. et al. Inorganic carbon dynamics and their relation to autotrophic community regime shift over three decades in a large, alkaline river. *Limnol. Oceanogr.* **70**, 1122–1136 (2025).
62. Hotchkiss, E. R. et al. Sources of and processes controlling CO2 emissions change with the size of streams and rivers. *Nat. Geosci.* **8**, 696–699 (2015).
63. Duvert, C., Butman, D. E., Marx, A., Ribolzi, O. & Hutley, L. B. CO2 evasion along streams driven by groundwater inputs and geomorphic controls. *Nat. Geosci.* **11**, 813–818 (2018).
64. Stets, E. G. et al. Carbonate buffering and metabolic controls on carbon dioxide in rivers. *Glob. Biogeochem. Cycles* **31**, 663–677 (2017).
65. Saccardi, B., Brinkerhoff, C. B., Gleason, C. J. & Winnick, M. J. Toward modeling continental-scale inland water carbon dioxide emissions. *AGU Adv.* **5**, e2024AV001294 (2024).
66. Borges, A. V. et al. Variations in dissolved greenhouse gases (CO_2, CH_4, N_2O) in the Congo River network overwhelmingly driven by fluvial-wetland connectivity. *Biogeosciences* **16**, 3801–3834 (2019).
67. Pace, M. L. & Prairie, Y. T. in *Respiration in Aquatic Ecosystems* 103–122 (Oxford Univ. Press, 2005).
68. Koehler, B., Landelius, T., Weyhenmeyer, G. A., Machida, N. & Tranvik, L. J. Sunlight-induced carbon dioxide emissions from inland waters. *Glob. Biogeochem. Cycles* **28**, 696–711 (2014).
69. Cory, R. M., McKnight, D. M., Chin, Y., Miller, P. & Jaros, C. L. Chemical characteristics of fulvic acids from Arctic surface waters: microbial contributions and photochemical transformations. *J. Geophys. Res.* **112**, 2006JG000343 (2007).
70. Maavara, T. et al. Does photomineralization of dissolved organics matter in temperate rivers? *J. Geophys. Res.* **126**, e2021JG006402 (2021).
71. Leng, P. & Koschorreck, M. Metabolism and carbonate buffering drive seasonal dynamics of CO2 emissions from two German reservoirs. *Water Res.* **242**, 120302 (2023).
72. Khan, H., Marcé, R., Laas, A. & Obrador, B. The relevance of pelagic calcification in the global carbon budget of lakes and reservoirs. *Limnetica* **41**, 17–25 (2022).
73. Grasset, C., Mesman, J. P., Tranvik, L. J., Maranger, R. & Sobek, S. Contribution of lake littoral zones to the continental carbon budget. *Nat. Geosci.* **18**, 747–752 (2025).
74. Bastviken, D., Cole, J. J., Pace, M. L. & Van De Bogert, M. C. Fates of methane from different lake habitats: connecting whole-lake budgets and CH_4 emissions. *J. Geophys. Res.* **113**, 2007JG000608 (2008).
75. Hartmann, J. F. et al. High spatiotemporal dynamics of methane production and emission in oxic surface water. *Environ. Sci. Technol.* **54**, 1451–1463 (2020).
76. Bižić, M. et al. Aquatic and terrestrial cyanobacteria produce methane. *Sci. Adv.* **6**, eaax5343 (2020).
77. Olid, C. et al. Groundwater discharge as a driver of methane emissions from Arctic lakes. *Nat. Commun.* **13**, 3667 (2022).
78. Schenk, J. et al. Methane in lakes: variability in stable carbon isotopic composition and the potential importance of groundwater input. *Front. Earth Sci.* **9**, 722215 (2021).
79. West, W. E., Creamer, K. P. & Jones, S. E. Productivity and depth regulate lake contributions to atmospheric methane. *Limnol. Oceanogr.* **61**, S51–S61 (2016).
80. Bastviken, D. et al. The importance of plants for methane emission at the ecosystem scale. *Aquat. Bot.* **184**, 103596 (2023).
81. DelSontro, T. et al. Spatial heterogeneity of methane ebullition in a large tropical reservoir. *Environ. Sci. Technol.* **45**, 9866–9873 (2011).
82. Beaulieu, J. J., McManus, M. G. & Nietch, C. T. Estimates of reservoir methane emissions based on a spatially balanced probabilistic-survey. *Limnol. Oceanogr.* **61**, S27–S40 (2016).
83. Walter, K. M., Zimov, S. A., Chanton, J. P., Verbyla, D. & Chapin, F. S. Methane bubbling from Siberian thaw lakes as a positive feedback to climate warming. *Nature* **443**, 71–75 (2006).
84. Kuhn, M. A. et al. High ebullitive, millennial-aged greenhouse gas emissions from thermokarst expansion of peatland lakes in boreal western Canada. *Limnol. Oceanogr.* **68**, 498–513 (2023).

85. Cunada, C. L., Lesack, L. F. W. & Tank, S. E. Methane emission dynamics among CO_2-absorbing and thermokarst lakes of a great Arctic delta. *Biogeochemistry* **156**, 375–399 (2021).
86. Mu, C. et al. Methane emissions from thermokarst lakes must emphasize the ice-melting impact on the Tibetan Plateau. *Nat. Commun.* **16**, 2404 (2025).
87. Guo, M. et al. Linking biogeochemical and hydrodynamic processes to model methane fluxes in shallow, tropical floodplain lakes. *J. Adv. Model. Earth Syst.* **15**, e2022MS003385 (2023).
88. Teodoru, C. R. et al. The net carbon footprint of a newly created boreal hydroelectric reservoir. *Glob. Biogeochem. Cycles* **26**, 2011GB004187 (2012).
89. Stanley, E. H. et al. The ecology of methane in streams and rivers: patterns, controls, and global significance. *Ecol. Monogr.* **86**, 146–171 (2016).
90. Crawford, J. T. et al. Ebullitive methane emissions from oxygenated wetland streams. *Glob. Change Biol.* **20**, 3408–3422 (2014).
91. Lupon, A. et al. Groundwater inflows control patterns and sources of greenhouse gas emissions from streams. *Limnol. Oceanogr.* **64**, 1545–1557 (2019).
92. Balathandayuthabani, S., Wallin, M. B., Klemedtsson, L., Crill, P. & Bastviken, D. Aquatic carbon fluxes in a hemiboreal catchment are predictable from landscape morphology, temperature, and runoff. *Limnol. Oceanogr. Lett.* **8**, 313–322 (2023).
93. Natchimuthu, S., Wallin, M. B., Klemedtsson, L. & Bastviken, D. Spatio-temporal patterns of stream methane and carbon dioxide emissions in a hemiboreal catchment in Southwest Sweden. *Sci. Rep.* **7**, 39729 (2017).
94. Balathandayuthabani, S. et al. Methane in two stream networks: similar contributions from groundwater and local sediments while oxidation was a large sink controlling atmospheric emissions. *J. Geophys. Res.* **129**, e2023JG007836 (2024).
95. Zhu, Y. et al. Separating natural from human enhanced methane emissions in headwater streams. *Nat. Commun.* **13**, 3810 (2022).
96. Niu, X. et al. Quantifying the contribution of methane diffusion and ebullition from agricultural ditches. *Sci. Total Environ.* **919**, 170912 (2024).
97. Ye, F., Zhu, Q., Cotta, S. R., Li, X. & Wang, Y. Methane from urban river networks: distinct responses of methanogenic pathways to substrate stimulation. *Sci. Total Environ.* **999**, 180369 (2025).
98. Zhao, F. et al. Oxic urban rivers as a potential source of atmospheric methane. *Environ. Pollut.* **297**, 118769 (2022).
99. Wang, G. et al. Intense methane ebullition from urban inland waters and its significant contribution to greenhouse gas emissions. *Water Res.* **189**, 116654 (2021).
100. Thottathil, S. D., Reis, P. C. J., Del Giorgio, P. A. & Prairie, Y. T. The extent and regulation of summer methane oxidation in northern lakes. *J. Geophys. Res.* **123**, 3216–3230 (2018).
101. Bastviken, D. in *Encyclopedia of Inland Waters* 136–154, https://doi.org/10.1016/B978-0-12-819166-8.00147-X (Elsevier, 2022).
102. Whalen, S. C. Biogeochemistry of methane exchange between natural wetlands and the atmosphere. *Environ. Eng. Sci.* **22**, 73–94 (2005).
103. D'Ambrosio, S. L. & Harrison, J. A. Methanogenesis exceeds CH_4 consumption in eutrophic lake sediments. *Limnol. Oceanogr. Lett.* **6**, 173–181 (2021).
104. Sawakuchi, H. O. et al. Phosphorus regulation of methane oxidation in water from ice-covered lakes. *J. Geophys. Res.* **126**, e2020JG006190 (2021).
105. Pajala, G. et al. Higher apparent gas transfer velocities for CO_2 compared to CH_4 in small lakes. *Environ. Sci. Technol.* **57**, 8578–8587 (2023).
106. Reis, P. C. J., Thottathil, S. D. & Prairie, Y. T. The role of methanotrophy in the microbial carbon metabolism of temperate lakes. *Nat. Commun.* **13**, 43 (2022).
107. McGinnis, D. F., Greinert, J., Artemov, Y., Beaubien, S. E. & Wüest, A. Fate of rising methane bubbles in stratified waters: how much methane reaches the atmosphere? *J. Geophys. Res.* **111**, 2005JC003183 (2006).
108. Strock, K. E., Krewson, R. B., Hayes, N. M. & Deemer, B. R. Oxidation is a potentially significant methane sink in land-terminating glacial runoff. *Sci. Rep.* **14**, 23389 (2024).
109. Sawakuchi, H. O. et al. Oxidative mitigation of aquatic methane emissions in large Amazonian rivers. *Glob. Change Biol.* **22**, 1075–1085 (2016).
110. Robison, A. L. et al. Dominance of diffusive methane emissions from lowland headwater streams promotes oxidation and isotopic enrichment. *Front. Environ. Sci.* **9**, 791305 (2022).
111. Baulch, H. M., Dillon, P. J., Maranger, R. & Schiff, S. L. Diffusive and ebullitive transport of methane and nitrous oxide from streams: are bubble-mediated fluxes important? *J. Geophys. Res.* **116**, G04028 (2011).
112. Varadharajan, C. & Hemond, H. F. Time-series analysis of high-resolution ebullition fluxes from a stratified, freshwater lake. *J. Geophys. Res.* **117**, 2011JG001866 (2012).
113. Wang, J. et al. Inland waters increasingly produce and emit nitrous oxide. *Environ. Sci. Technol.* **57**, 13506–13519 (2023).
114. Turner, P. A. et al. Indirect nitrous oxide emissions from streams within the US Corn Belt scale with stream order. *Proc. Natl Acad. Sci. USA* **112**, 9839–9843 (2015).
115. Hu, M. et al. Hydrologic connectivity regulates riverine N_2O sources and dynamics. *Environ. Sci. Technol.* **58**, 9701–9713 (2024).
116. Wang, S. et al. Author correction: ammonium-derived nitrous oxide is a global source in streams. *Nat. Commun.* **15**, 4543 (2024).
117. Beaulieu, J. J. et al. Nitrous oxide emission from denitrification in stream and river networks. *Proc. Natl Acad. Sci. USA* **108**, 214–219 (2011).
118. Guilhen, J. et al. Denitrification and associated nitrous oxide and carbon dioxide emissions from the Amazonian wetlands. *Biogeosciences* **17**, 4297–4311 (2020).
119. Yu, J. et al. Is the impact of groundwater on lake greenhouse gas dynamics underestimated? A comparative analysis of subsurface and ecological factors. *J. Hydrol.* **640**, 131666 (2024).
120. Beaulieu, J. J., Nietch, C. T. & Young, J. L. Controls on nitrous oxide production and consumption in reservoirs of the Ohio River Basin. *J. Geophys. Res.* **120**, 1995–2010 (2015).
121. Mengis, M., Gächter, R. & Wehrli, B. Sources and sinks of nitrous oxide (N2O) in deep lakes. *Biogeochemistry* **38**, 281–301 (1997).
122. Mosier, A. et al. Closing the global N2O budget: nitrous oxide emissions through the agricultural nitrogen cycle. *Nutr. Cycl. Agroecosystems* **52**, 225–248 (1998).
123. Vachon, D., Prairie, Y. T., Guillemette, F. & Del Giorgio, P. A. Modeling allochthonous dissolved organic carbon mineralization under variable hydrologic regimes in boreal lakes. *Ecosystems* **20**, 781–795 (2017).
124. Hutchins, R. H. S., Casas-Ruiz, J. P., Prairie, Y. T. & Del Giorgio, P. A. Magnitude and drivers of integrated fluvial network greenhouse gas emissions across the boreal landscape in Québec. *Water Res.* **173**, 115556 (2020).
125. Hastie, A. et al. CO_2 evasion from boreal lakes: revised estimate, drivers of spatial variability, and future projections. *Glob. Change Biol.* **24**, 711–728 (2018).
126. Campeau, A. et al. Current forest carbon fixation fuels stream CO_2 emissions. *Nat. Commun.* **10**, 1876 (2019).
127. Lauerwald, R., Regnier, P., Guenet, B., Friedlingstein, P. & Ciais, P. How simulations of the land carbon sink are biased by ignoring fluvial carbon transfers: a case study for the Amazon basin. *One Earth* **3**, 226–236 (2020).
128. Zhang, H. et al. Global changes alter the amount and composition of land carbon deliveries to European rivers and seas. *Commun. Earth Environ.* **3**, 245 (2022).
129. Saros, J. E. et al. Sentinel responses of Arctic freshwater systems to climate: linkages, evidence, and a roadmap for future research. *Arct. Sci.* **9**, 356–392 (2023).
130. Kosten, S. et al. Climate-dependent CO_2 emissions from lakes. *Glob. Biogeochem. Cycles* **24**, 2009GB003618 (2010).
131. De Fátima, F. L. et al. Spatial and temporal variability of pCO2 and CO2 efflux in seven Amazonian Rivers. *Biogeochemistry* **116**, 241–259 (2013).
132. Xu, Y. J., Xu, Z. & Potter, L. Connectivity of floodplain influences riverine carbon outgassing and dissolved carbon transport. *Sci. Total Environ.* **924**, 171604 (2024).
133. Limpert, K. E., Carnell, P. E., Trevathan-Tackett, S. M. & Macreadie, P. I. Reducing emissions from degraded floodplain wetlands. *Front. Environ. Sci.* **8**, 8 (2020).
134. Bowring, S. P. K. et al. ORCHIDEE MICT-LEAK (r5459), a global model for the production, transport, and transformation of dissolved organic carbon from Arctic permafrost regions – part 2: model evaluation over the Lena River basin. *Geosci. Model Dev.* **13**, 507–520 (2020).
135. Serikova, S. et al. High riverine CO2 emissions at the permafrost boundary of Western Siberia. *Nat. Geosci.* **11**, 825–829 (2018).
136. Nydahl, A. C., Wallin, M. B. & Weyhenmeyer, G. A. No long-term trends in pCO_2 despite increasing organic carbon concentrations in boreal lakes, streams, and rivers. *Glob. Biogeochem. Cycles* **31**, 985–995 (2017).
137. Park, J.-H. et al. Reviews and syntheses: anthropogenic perturbations to carbon fluxes in Asian river systems – concepts, emerging trends, and research challenges. *Biogeosciences* **15**, 3049–3069 (2018).
138. Bednařík, A., Bodmer, P., Darenova, E., Kokrda, L. & Pavelka, M. Temperature, water depth, and flow velocity are important drivers of methane ebullition in a temperate lowland stream. *J. Geophys. Res.* **129**, e2023JG007597 (2024).
139. Deemer, B. R. et al. Greenhouse gas emissions from reservoir water surfaces: a new global synthesis. *BioScience* **66**, 949–964 (2016).
140. Beaulieu, J. J., DelSontro, T. & Downing, J. A. Eutrophication will increase methane emissions from lakes and impoundments during the 21st century. *Nat. Commun.* **10**, 1375 (2019).
141. Pi, X. et al. Mapping global lake dynamics reveals the emerging roles of small lakes. *Nat. Commun.* **13**, 5777 (2022).
142. St. Louis, V. L., Kelly, C. A., Duchemin, É, Rudd, J. W. M. & Rosenberg, D. M. Reservoir surfaces as sources of greenhouse gases to the atmosphere: a global estimate. *BioScience* **50**, 766 (2000).
143. Almeida, R. M. et al. Reducing greenhouse gas emissions of Amazon hydropower with strategic dam planning. *Nat. Commun.* **10**, 4281 (2019).
144. Barros, N. et al. Carbon emission from hydroelectric reservoirs linked to reservoir age and latitude. *Nat. Geosci.* **4**, 593–596 (2011).
145. Walter Anthony, K. et al. Methane emissions proportional to permafrost carbon thawed in Arctic lakes since the 1950s. *Nat. Geosci.* **9**, 679–682 (2016).
146. Prėskienis, V. et al. Seasonal patterns in greenhouse gas emissions from lakes and ponds in a high Arctic polygonal landscape. *Limnol. Oceanogr.* **66**, S1–S426 (2021).
147. Wik, M., Varner, R. K., Anthony, K. W., MacIntyre, S. & Bastviken, D. Climate-sensitive northern lakes and ponds are critical components of methane release. *Nat. Geosci.* **9**, 99–105 (2016).
148. Zhang, L. et al. Significant methane ebullition from alpine permafrost rivers on the East Qinghai–Tibet Plateau. *Nat. Geosci.* **13**, 349–354 (2020).
149. Levenson, E. S., Cooley, S., Mullen, A., Webb, E. E. & Watts, J. Glacial history modifies permafrost controls on the distribution of lakes and ponds. *Geophys. Res. Lett.* **52**, e2024GL112771 (2025).
150. Webb, E. E. & Liljedahl, A. K. Diminishing lake area across the northern permafrost zone. *Nat. Geosci.* **16**, 202–209 (2023).
151. Webb, J. R. et al. Widespread nitrous oxide undersaturation in farm waterbodies creates an unexpected greenhouse gas sink. *Proc. Natl Acad. Sci. USA* **116**, 9814–9819 (2019).
152. Kortelainen, P. et al. Lakes as nitrous oxide sources in the boreal landscape. *Glob. Change Biol.* **26**, 1432–1445 (2020).

153. Velthuis, M. & Veraart, A. J. Temperature sensitivity of freshwater denitrification and N_2O emission—a meta-analysis. *Glob. Biogeochem. Cycles* **36**, e2022GB007339 (2022).
154. Chun, Y. et al. Temperature control on wastewater and downstream nitrous oxide emissions in an urbanized river system. *Water Res.* **187**, 116417 (2020).
155. Gergel, S. E., Carpenter, S. R. & Stanley, E. H. Do dams and levees impact nitrogen cycling? Simulating the effects of flood alterations on floodplain denitrification. *Glob. Change Biol.* **11**, 1352–1367 (2005).
156. Regnier, P. et al. Anthropogenic perturbation of the carbon fluxes from land to ocean. *Nat. Geosci.* **6**, 597–607 (2013).
157. IPCC. *Climate Change 2021 – The Physical Science Basis: Working Group I Contribution to the Sixth Assessment Report of the Intergovernmental Panel on Climate Change* https://doi.org/10.1017/9781009157896 (Cambridge Univ. Press, 2021).
158. Hastie, A., Lauerwald, R., Ciais, P., Papa, F. & Regnier, P. Historical and future contributions of inland waters to the Congo Basin carbon balance. *Earth Syst. Dyn.* **12**, 37–62 (2021).
159. Wang, S. et al. Recent global decline of CO_2 fertilization effects on vegetation photosynthesis. *Science* **370**, 1295–1300 (2020).
160. Madani, N. et al. Future global productivity will be affected by plant trait response to climate. *Sci. Rep.* **8**, 2870 (2018).
161. Müller, O. V., McGuire, P. C., Vidale, P. L. & Hawkins, E. River flow in the near future: a global perspective in the context of a high-emission climate change scenario. *Hydrol. Earth Syst. Sci.* **28**, 2179–2201 (2024).
162. Fleischmann, A. S. et al. Increased floodplain inundation in the Amazon since 1980. *Environ. Res. Lett.* **18**, 034024 (2023).
163. Thoman, R. L. et al. The Arctic. *Bull. Am. Meteorol. Soc.* **106**, S300–S356 (2025).
164. Zarfl, C., Lumsdon, A. E., Berlekamp, J., Tydecks, L. & Tockner, K. A global boom in hydropower dam construction. *Aquat. Sci.* **77**, 161–170 (2015).
165. Schmitt, R. J. P. & Rosa, L. Dams for hydropower and irrigation: trends, challenges, and alternatives. *Renew. Sustain. Energy Rev.* **199**, 114439 (2024).
166. Sillen, S. J., Ross, M. R. V. & Collins, S. M. Long-term trends in productivity across intermountain west lakes provide no evidence of widespread eutrophication. *Water Resour. Res.* **60**, e2023WR034997 (2024).
167. Cloern, J. E. & Jassby, A. D. Chlorophyll trends are negative for lakes but positive for estuarine–coastal waters. *Proc. Natl Acad. Sci. USA* **122**, e2502289122 (2025).
168. Yan, X., Thieu, V. & Garnier, J. Long-term evolution of greenhouse gas emissions from global reservoirs. *Front. Environ. Sci.* **9**, 705477 (2021).
169. Sikder, M. S. et al. Lake-TopoCat: a global lake drainage topology and catchment database. *Earth Syst. Sci. Data* **15**, 3483–3511 (2023).
170. Sartori, M. et al. Remaining loyal to our soil: a prospective integrated assessment of soil erosion on global food security. *Ecol. Econ.* **219**, 108103 (2024).
171. Hu, M., Chen, D. & Dahlgren, R. A. Modeling nitrous oxide emission from rivers: a global assessment. *Glob. Change Biol.* **22**, 3566–3582 (2016).
172. Sø, J. S., Sand-Jensen, K. & Kragh, T. Self-made equipment for automatic methane diffusion and ebullition measurements from aquatic environments. *J. Geophys. Res.* **129**, e2024JG008035 (2024).
173. Bastviken, D., Sundgren, I., Natchimuthu, S., Reyier, H. & Gålfalk, M. Technical note: cost-efficient approaches to measure carbon dioxide (CO_2) fluxes and concentrations in terrestrial and aquatic environments using mini loggers. *Biogeosciences* **12**, 3849–3859 (2015).
174. Manning, C. C. et al. River inflow dominates methane emissions in an arctic coastal system. *Geophys. Res. Lett.* **47**, e2020GL087669 (2020).
175. Gålfalk, M., Nilsson Påledal, S. & Bastviken, D. Sensitive drone mapping of methane emissions without the need for supplementary ground-based measurements. *ACS Earth Space Chem.* **5**, 2668–2676 (2021).
176. Bolek, A., Heimann, M. & Göckede, M. UAV-based in situ measurements of CO_2 and CH_4 fluxes over complex natural ecosystems. *Atmos. Meas. Tech.* **17**, 5619–5636 (2024).
177. Friedlingstein, P. et al. Global carbon budget 2020. *Earth Syst. Sci. Data* **12**, 3269–3340 (2020).

Acknowledgements

R.L. acknowledges funding from French state aid, managed by ANR under the 'Investissements d'avenir' programme (ANR-16-CONV-0003) and under the 'France 2030' programme (ANR-22-PEXF-0009, PEPR FairCarboN — project 'DEEP-C'). A. M. acknowledges funding from the Italian Ministry of Education, University and Research (MIUR) in the frame of the Departments of Excellence Initiative 2023–2027, granted to the Department of Civil, Environmental and Mechanical Engineering of the University of Trento. D.B. acknowledges support from the Swedish Research Council VR (2022-03841), the Knut and Alice Wallenberg Foundation (RELITORATE) and Linköping University. L.R. acknowledges support from the Research Grants Council of Hong Kong (C7002-24GF). G.A. acknowledges support from CNRS Ecology and Environment through the International Research Project VELITROP and International Research Laboratory MAREL. N.C. acknowledges support from the Spanish Ministry of Science and Universities (PID2022-140848NB-C32). Any use of trade, firm or product names is for descriptive purposes only and does not imply endorsement by the US Government.

Author contributions

R.L. and P.R. developed the concept of the paper and researched data for the article. R.L. performed the data analysis and designed the original figures. All authors contributed substantially to discussions of the content, contributed to writing the article, and reviewed and/or edited the manuscript before submission.

Competing interests

The authors declare no competing interests.

Additional information

Supplementary information The online version contains supplementary material available at https://doi.org/10.1038/s43017-026-00818-7.

Peer review information *Nature Reviews Earth & Environment* thanks Ralf C. H. Aben and the other, anonymous, reviewer(s) for their contribution to the peer review of this work.

Publisher's note Springer Nature remains neutral with regard to jurisdictional claims in published maps and institutional affiliations.

Springer Nature or its licensor (e.g. a society or other partner) holds exclusive rights to this article under a publishing agreement with the author(s) or other rightsholder(s); author self-archiving of the accepted manuscript version of this article is solely governed by the terms of such publishing agreement and applicable law.

© The Authors. Parts of this work were authored by US Federal Government authors and are not under copyright protection in the US; foreign copyright protection may apply. 2026

[1]Université Paris-Saclay, INRAE/AgroParisTech — UMR EcoSys, Palaiseau, France. [2]Linköping University, Department of Thematic Studies — Environmental Change, Linköping, Sweden. [3]École Polytechnique Fédérale de Lausanne, River Ecosystems Laboratory, Alpine and Polar Environmental Research Centre (ALPOLE), Lausanne, Switzerland. [4]CEA/CNRS/UVSQ — Laboratoire des Sciences du Climat et de l'Environnement, Université Paris-Saclay, Gif-sur-Yvette, France. [5]Boston College, Department of Earth and Environmental Sciences,Center for Earth System Science and Global Sustainability, Schiller Institute for Integrated Science and Society, Chestnut Hill, MA, USA. [6]Virginia Polytechnic Institute and State University, Department of Geosciences, Blacksburg, VA, USA. [7]Marine Eutrophication Laboratory, CNRS, UERJ, UFF, Rio de Janeiro, Brazil. [8]CEAB-CSIC, Integrative Freshwater Ecology Group, Center for Advanced Studies of Blanes, Blanes, Spain. [9]U.S. Geological Survey, Southwest Biological Science Center, Grand Canyon Monitoring and Research Center, Flagstaff, AZ, USA. [10]University of Trento, Department of Civil, Environmental and Mechanical Engineering, Trento, Italy. [11]Université du Québec à Montréal, Department of Biological Sciences, Montréal, Québec, Canada. [12]University of Alberta, Department of Biological Sciences, Edmonton, Alberta, Canada. [13]Purdue University, Department of Earth, Atmospheric and Planetary Sciences, West Lafayette, IN, USA. [14]University of Hong Kong, Department of Geography, Hong Kong, China. [15]Commonwealth Scientific and Industrial Research Organisation (CSIRO), Canberra, Australian Capital Territory, Australia. [16]Université Libre de Bruxelles, Department Geoscience, Environment and Society-BGEOSYS, Brussels, Belgium.